EFFECT OF BRANCHING PROCESSES ON THE GLOW OF THE DISCHARGE CHANNEL DURING BREAKDOWN IN A HIGHLY NONUNIFORM FIELD

M. F. Danilov

UDC 537.521.7

The branching of a discharge channel is certainly part of breakdown processes in a long spark gap. This is evidenced by photographs of lightning, a long spark in air, and a creeping spark on the surface of a dielectric [1-4]. Data on branching processes have been presented most fully in [1]. The information about them in [2-7] is less detailed, and as a rule attention is centered on the time characteristics of the processes, which are discussed within the framework of one-dimensional models. Creeping-spark studies [8, 9] revealed that the discharge-channel glow has a longitudinal nonuniformity which arises in the initial phase of the breakdown, is absent near the maximum of the bulk current, and then reappears in the final stage of the discharge. We note that it is spatially linked to the channel-branch points. A nonuniform glow is also observed during a lightning discharge near bends in the channel in the final stage of the main discharge [1]. In view of this, attention must be focused on the fact that side branches often run from the bend points.

We consider the model of a space-charge sheath with allowance for the branching processes. The model is used to calculate the electric field in the branching region and an explanation is given for the longitudinal nonuniformity of the discharge-channel glow in a long spark gap.

The diccussion is confined to relatively slow processes when we can disregard the vortex component of the field which is comparable with the potential component only when the current changes at a rate exceeding 10^{10} A/sec [6]. The electric field strength E in the discharge zone is then determined by the volume density ρ of the electric charge, according to the Poisson equation

$$\operatorname{div} \mathbf{E} = \rho/\varepsilon_0 \tag{1}$$

(ε_0 is the electric constant). The space-charge distribution is formed in accordance with the continuity equation

$$\partial\rho/\partial t + \operatorname{div} \mathbf{j} = 0 \tag{2}$$

($\mathbf{j} = \sigma \mathbf{E}$ is the current density and σ is the electrical conductivity). Using (1), we recast Eq. (2) in the form

$$\partial\rho/\partial t + \operatorname{grad} \sigma \cdot \mathbf{E} + \rho\sigma/\varepsilon_0 = 0. \tag{3}$$

The scalar product $\operatorname{grad}\sigma \cdot \mathbf{E}$ determines the process whereby the charge increases at the boundary of the conducting channel, where $\operatorname{grad}\sigma \cdot \mathbf{E} < 0$. At the same time in the zone of high conductivity the space charge relaxes with a characteristic time $\tau = \varepsilon_0/\sigma \sim 10^{-14}$ sec. The charge density in this case tends asymptotically to $\rho_0 = -\operatorname{grad}\sigma \cdot \mathbf{E}\varepsilon_0/\sigma$. Estimates show that ρ_0 is several orders of magnitude smaller than the charge density in the sheath. Streamer [5, 6] and autowave charge-transfer processes also participate in the formation of the space-charge sheath. They are initiated in the region of high-field strength near the channel boundary and then develop outside that zone, smearing the region of charge localization. As a result, the space-charge layer becomes substantially thicker and the field strength at the channel boundary decreases.

First we consider the sheath structure when there is no branching and then the changes that take place in this structure when side branches appear. No experimental data on the charge distribution in the sheath are available. We assume, therefore, that the average charge density depends on the coordinates as

Sosnovyi Bor. Translated from Zhurnal Prikladnoi Mekhaniki i Tekhnicheskoi Fiziki, No. 4, pp. 10-13, July-August, 1991. Original article submitted August 7, 1989; revision submitted April 4, 1990.

 0021-8944/91/3204-0472$12.50

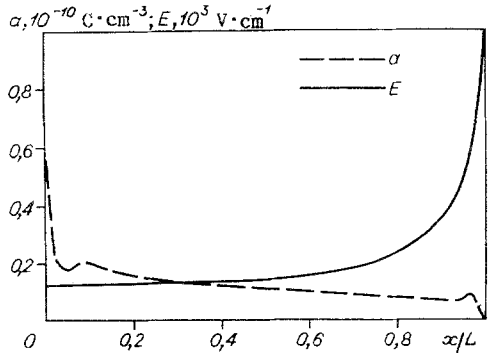

Fig. 1

$$\rho(x, y) = \begin{cases} p_1 a(x), & y = y_0, \\ a(x) \exp\left(-(y - y_0)^2 / r_s^2\right), & y \neq y_0. \end{cases} \quad (4)$$

Here x and y are the coordinates in the direction along and across the axis of the discharge channel, respectively; the channel axis coincides with the straight line $y = y_0$ and r_s is of the same order of magnitude as the radius of the streamer zone. The parameter $p_1 < 1$ shows that the average charge density in the region of the channel is lower than in the other part of the sheath surrounding it. For simplicity we assume that with respect to the third coordinate z the charge is concentrated in a thin layer and its distribution is described by the Dirac δ function. This assumption can be substantiated by the fact that preferential directions of charge development along the plane of the surface exist under certain conditions. Such a situation occurs, e.g., when a creeping discharge develops along the boundary between a gas and a solid dielectric. We estimate the nature of the charge distribution in the longitudinal direction, i.e., find $a(x)$, by using the dependence of the electric field in the discharge channel of a long spark on the coordinate x [5], for which the field strength and potential can be described approximately by the formulas

$$E(x) = b/(L - x) + c; \quad (5)$$

$$\varphi(x) = b \ln (L - x) - cx + f \quad (6)$$

(b, c, and f are constants and L is the channel length).

Adopting the model of the charge distribution (4) and the potential of the electric field (6) and solving the electrostatic problem for the charge distribution, we find $a(x)$. Figure 1 shows an example of calculation of $a(x)$ and gives the results of calculation of the field strength E(x) for the charge distribution obtained. The field potential was calculated by the convolution method [10] and the field strength, from the formula $E = -\text{grad}\,\varphi$. The distribution of an isolated system [10] of space charges $\rho(x, y)$ was given on a 32×32 net. The results of the calculation confirm that the charge distribution obtained is consistent with the initial conditions of the problem (5), (6).

We now go on to discuss the branching processes. The lack of a bulk conduction current is a characteristic feature of the incomplete stage of breakdown in a long spark gap. The current in the external circuit should be treated as a bias current [5]. In other words, the conduction current in the discharge channel is closed by bias currents in the space surrounding the channel [9]. Conductivity in the breakdown zone varies from $\sigma \sim 10^{-14}$ S [11], which is a typical value for air under normal conditions, to $\sigma \sim 10^3$-10^4 S [1, 3, 5], which is typical of the leader channel in air. From the ratio of the conduction current density to the bias current [12] $j/j_c \sim \sigma/\varepsilon_0\omega$ for a large frequency range ($\omega \sim 10^{-2}$-10^{13} sec^{-1}) we find that $j_c \ll j$ in the discharge channel and $j \ll j_c$ in the unperturbed space surrounding the channel. The streamer zone can be regarded as a region where $j \sim j_c$. In a nonlinear medium it is energetically more convenient for the conduction current to flow in narrow channels at a high current density and high conductivity [13], which is manifested by contraction. The bias current, by contrast, depends little on the properties of the medium and is proportional to the effective area of the lateral surface of the discharge channel. In order to ensure that the conduction current and the bias current are equal in the incomplete stage, the narrow conducting channel should branch, increasing the areas of its lateral surface. An exception are discharges (or individual parts of them) produced at high

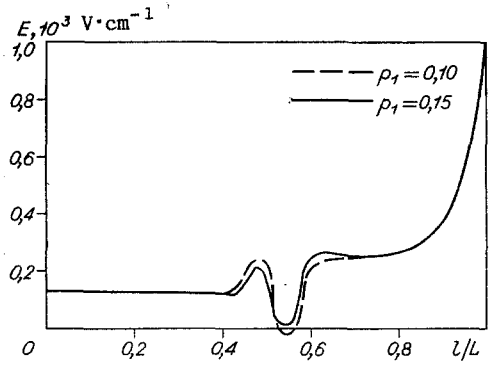

Fig. 2

values of dU/dt, when breakdown develops without branching since the rapid growth of the voltage ensures the necessary value of bias current. The appearance of a side branch causes changes in the structure of the sheath of the main channel, which reduce mainly to a decrease in the charge density in the zone around the axis of the side channel. We assume that the side branch has the same kind of charge distribution in the sheath as in the main channel, but they may be of different lengths. This can be taken into account, e.g., by introducing a scaling factor for the coordinate ℓ, measured along the channel axis. The charge-distribution model then has the form

$$\rho(x, y) = \begin{cases} p_1 a(p_2 l), & d < r_c, \\ a(p_2 l) \exp\left(-d^2/r_s^2\right), & d \geqslant r_c, \end{cases} \tag{7}$$

where p_2 is the scaling factor, $p_2 = 1$ for the main channel and $p_2 \geq 1$ for the side channel; d is the minimum distance from the point x, y to the axis of the main or side channel; in the general case r_c depends on the angle α between the axes of the main channel and side branch: $r_{ch} \leq r_c < (\Delta x + \Delta y)/4$; r_{ch} is the channel radius; and Δx and Δy are the spacings of the coordinate net. The changes in the structure of the space-charge sheath should affect the value of the electric field. This assumption is supported by calculation of the field strength carried out for the charge distribution (7) with allowance for the channel branching. Calculation shows that the dependence of the field on the coordinate ℓ on the axis of the main channel ceases to be monotonic. Near a branch point it undergoes modulation, which is observed over a wide range of charge-distribution parameters (7) (r_s, p_1, p_2, and r_c were varied). We considered channels with one branch point, having one or two symmetrically arranged side branches. Figure 2 shows examples of calculations of the field in the channel for the following parameters of the model: $p_1 = 0.1$, 0.15, $p_2 = 4.0$, $r_s = L/32$, and $r_c = L/3200$. Two side channels emerge at an angle $\alpha = 45°$ from the branch point with the coordinate $\ell \approx 0.5$ L.

Since the density of the energy released in the discharge per unit time is $W = \sigma E^2$, the spatial modulation of the field strength should result in the modulation of the channel glow. This can explain the longitudinal nonuniformity of the flow and the beaded structure described in [9]. Naturally, such a glow structure cannot be steady-state since modulation of the electric field causes modulation of the conduction current and this leads to a redistribution of the charge and a change in the channel glow. Indeed, the length of the bright segments in the incomplete stage increases with time, but the glow does not become entirely even [9]. As a rule, a less bright segment, which can be identified with the region of lower field strength near the point $\ell \approx 0.55$ L in Fig. 2, can be observed near a branch point. The branching channel formed during the incomplete stage of the breakdown undergoes further substantial changes but in all likelihood continues to exist, preserving its principal geometrical parameters until the breakdown is completed. The linkage of the long-glow segments of the channel to the spatial structure of the glow of the incomplete discharge, therefore, is attributable to the effect of the sheath of the residual space charge as well as to gasdynamic perturbations initiated in the region of the branching [9].

In conclusion, we must point out that the system of side branches, having a considerably lower brightness than the main channel has, is often not recorded experimentally but it can nevertheless play a significant role in the formation of the space-charge distribution and thus affect the energy processes in the discharge channel.

LITERATURE CITED

1. J. M. Meek and J. D. Craggs, Electrical Breakdown of Gases, UMI, North Carolina (1960).
2. I. S. Stekol'nikov, The Nature of a Long Spark [in Russian], Izd. Akad. Nauk SSSR, Moscow (1960).
3. M. A. Uman, Understanding Lightning, Bek Tech., Pittsburgh, PA (1971).
4. S. I. Andreev, E. A. Zobov, and A. N. Sidorov, "Creeping sparks in air," Prikl. Mekh. Tekh. Fiz., No. 3 (1978).
5. É. M. Bazelyan, "Leader of a positive long spark," Elektrichestvo, No. 5 (1987).
6. É. M. Bazelyan and I. M. Razhanskii, Spark Discharges in Air [in Russian], Nauka, Novosibirsk (1988).
7. B. N. Gorin, "Computational modeling of the main stage of lightning," Elektrichestvo, No. 4 (1985).
8. M. F. Borisov, M. F. Danilov, E. A. Zobov, et al., "Distinctive features of the spatial and temporal structure of the radiation of a creeping-spark channel," Abstracts of Papers Read at the 3rd All-Union Conf. on the Physics of Gas Discharges [in Russian], Part 1, Kiev. Gos. Univ., Kiev (1986).
9. M. F. Borisov, M. F. Danilov, E. A. Zobov, et al., "Structure of the discharge channel during breakdown in a nonuniform field," Prikl. Mekh. Tekh. Fiz., No. 6 (1988).
10. R. W. Hockney and J. W. Eastwood, Computer Simulation Using Particles, Taylor and Francis (1988).
11. Yu. V. Koritskii, V. V. Pasynkov, and B. M. Tareev (eds.), Handbook of Electrical Materials [in Russian], Vol. 1, Énergiya, Moscow (1974).
12. I. E. Tamm, Fundamentals of the Theory of Electricity [in Russian], Nauka, Moscow (1976).
13. Yu. P. Raizer, Fundamentals of the Modern Physics of Gas-Discharge Processes [in Russian], Nauka, Moscow (1980).

MAGNETOACOUSTIC SHOCK WAVES IN A NONUNIFORM PLASMA FLOW

V. A. Pavlov

UDC 532.593

The flow of the solar wind around the planets and other bodies generates a weak magnetoacoustic shock wave [1]. The problem of describing a shock wave in a nonuniform plasma flow arises in this and similar situations [2]. Here we propose an approximate method of describing the field in the vicinity of a magnetoacoustic shock front. Based on the geometrical-acoustics (ray) description, this field is represented by a series, in which second-order small terms are taken into account by solving a Riccati equation. The magnetoacoustic shock intensity is estimated, and a relation is derived between the velocity of the shock front and the cross section of the ray tube. An algorithm is proposed for converting the fields from the moving frame to the laboratory frame.

1. We describe the field in the cold plasma by the magnetohydrodynamic (MHD) equations

$$\begin{gathered}\partial\rho/\partial t + \operatorname{div}(\rho\mathbf{v}) = 0,\ \operatorname{div}\mathbf{H} = 0,\\ \partial\mathbf{H}/\partial t - \operatorname{curl}[\mathbf{v}, \mathbf{H}] = 0,\ d\mathbf{v}/dt - (\mu/\rho)[\operatorname{curl}\mathbf{H}, \mathbf{H}] + \mathbf{g}(r) = 0.\end{gathered} \tag{1.1}$$

Here ρ, $\mathbf{v}$, and $\mathbf{H}$ are the density of the plasma, the velocity, and the magnetic field, and μ and $\mathbf{g}$ are the permeability and the gravitational acceleration. The subscript 0 refers to the unperturbed field: $\rho_0 = \rho_0(z)$, $\mathbf{v}_0 = v_0(z)\mathbf{e}_x$, $\mathbf{H}_0 = \text{const}$. The fields are perturbed by the presence of a fixed smooth body, around which the plasma moves in a nonuniform flow. We transform to a local coordinate system (frame) associated with the flow velocity $v_0(z)\mathbf{e}_x$ at

Leningrad. Translated from Zhurnal Prikladnoi Mekhaniki i Tekhnicheskoi Fiziki, No. 4, pp. 13-19, July-August, 1991. Original article submitted October 20, 1989; revision submitted March 16, 1990.

0021-8944/91/3204-0475$12.50